UT-ICEPP00-01

Precise Measurement of Cosmic-Ray Proton and Helium Spectra with the BESS Spectrometer

T. Sanuki[1], M. Motoki[2], H. Matsumoto[1], E. S. Seo[5], J. Z. Wang[5], K. Abe[1], K. Anraku[1], Y. Asaoka[1], M. Fujikawa[1], M. Imori[1], T. Maeno[1], Y. Makida[2], N. Matsui[1], H. Matsunaga[1], J. Mitchell[4], T. Mitsui[3], A. Moiseev[4], J. Nishimura[1], M. Nozaki[3], S. Orito[1], J. Ormes[4], T. Saeki[1], M. Sasaki[3], Y. Shikaze[1], T. Sonoda[1], R. Streitmatter[4], J. Suzuki[2], K. Tanaka[2], I. Ueda[1], N. Yajima[6], T. Yamagami[6], A. Yamamoto[2], T. Yoshida[2], and K. Yoshimura[1]

ABSTRACT

We report cosmic-ray proton and helium spectra in energy ranges of 1 to 120 GeV and 1 to 54 GeV/nucleon, respectively, measured by a balloon flight of the BESS spectrometer in 1998. The magnetic-rigidity of the cosmic-rays was reliably determined by highly precise measurement of the circular track in a uniform solenoidal magnetic field of 1 Tesla. Those spectra were determined within overall uncertainties of ± 5 % for protons and ± 10 % for helium nuclei including statistical and systematic errors.

Subject headings: cosmic rays

1. INTRODUCTION

The absolute fluxes and spectra of primary cosmic-ray protons and helium nuclei are fundamental information as references in cosmic-ray physics. They are needed to calculate secondary anti-protons, positrons, and diffuse gamma radiation, which in turn provide important knowledge of particle propagation and the matter distribution in interstellar space. Those are also indispensable for studying atmospheric neutrinos. Although measurement of the proton and helium energy

[1]Department of Physics, Faculty of Science, University of Tokyo, Bunkyo, Tokyo 113-0033, Japan; sanuki@icepp.s.u-tokyo.ac.jp

[2]High Energy Accelerator Research Organization (KEK), Tsukuba, Ibaraki 305-0801, Japan

[3]Kobe University, Kobe, Hyogo 657-8501, Japan

[4]National Aeronautics and Space Administration / Goddard Space Flight Center, Greenbelt, MD 20771, USA

[5]University of Maryland, College Park, MD 20742, USA

[6]The Institute of Space and Astronautical Science, Sagamihara, Kanagawa 229-8510, Japan

spectra has been performed in various experiments, their resultant absolute fluxes show discrepancies up to a factor of two at 50 GeV. This ambiguity causes large uncertainty in calculations of the atmospheric neutrinos, as well as secondary anti-protons, positrons, and diffuse gamma-rays.

We report a new precise measurement of the cosmic-ray proton and helium spectra over the energy ranges of 1 to 120 GeV for protons and 1 to 54 GeV/nucleon for helium nuclei, based on a half of the data from a BESS balloon flight in 1998. The covered energy range is relevant to the atmospheric neutrinos observed as "fully contained events" in Super-Kamiokande. In the BESS–98 flight, a new trigger mode was implemented with a silica-aerogel Cherenkov counter to record all energetic particles instead of sampling the protons at a ratio of 1/60 as done in the previous BESS flights. This drastically improved statistics in the high-energy region above 6 GeV/nucleon, as reported here.

2. THE BESS SPECTROMETER

The BESS detector is a high-resolution spectrometer with a large acceptance to perform highly sensitive searches for rare cosmic-ray components, as well as precise measurement of the absolute fluxes of various cosmic-ray particles (Orito 1987; Yamamoto et al. 1994; Ajima et al. 2000). As shown in Figure 1, all detector components are arranged in a simple cylindrical configuration with a thin superconducting solenoidal magnet. In the central region, the solenoid provides a uniform magnetic field of 1 Tesla (± 7 % in a fiducial volume). The trajectory of an incoming charged particle is measured by using the tracking system which consists of a central JET chamber and two inner drift chambers (IDC's) in a volume of 0.84 m in diameter and 1 m in length. The magnetic-rigidity ($R \equiv pc/Ze$) is reliably determined by a simple circular-fitting of the deflection (R^{-1}) using up-to 28 hit points each with a spatial resolution of 200 μm . Figure 2 shows the deflection uncertainty for protons evaluated in the track fitting procedure. Since the magnetic field is highly uniform, it has a narrow and sharp peak around 0.005, which corresponds to maximum detectable rigidity (MDR) of 200 GV, and has a small tail. The outermost detector is a set of time-of-flight (TOF) hodoscopes with 2 cm thick plastic scintillators. It provides the velocity ($\beta \equiv v/c$) and energy loss (dE/dx) measurements. The time resolution for energetic protons in each counter is 55 ps rms, resulting in a β^{-1} resolution of 1.4 %. The data acquisition sequence is initiated by a first-level TOF trigger by a simple coincidence of signals in the top and bottom scintillators, with the threshold level of 1/3 pulse height from minimum ionizing particles (MIP's). If the pulse height exceeds 2.5 times MIP signal, the TOF trigger is labeled as "helium-trigger," otherwise "proton-trigger." The TOF trigger efficiency was evaluated to be > 99.95 % from the muon data taken at sea level; thus, the systematic error caused by the TOF trigger inefficiency is negligibly small. In order to build a sample of unbiased triggers, one of every 60 and 25 "proton-triggered" and "helium-triggered" events, respectively, was recorded irrespective of succeeding online-selections.

The instrument has a threshold-type Cherenkov counter with a silica-aerogel radiator just below the top TOF hodoscope (Asaoka et al. 1998). The radiator was newly developed prior to the

BESS–98 flight and it has a refractive index of 1.022. An auxiliary trigger was generated by a signal from the Cherenkov counter to record all of the high energy particles above ~ 6 GeV without bias nor sampling. The efficiency of the Cherenkov trigger for the energetic particles was determined to be 92.1 ± 3.0 % by using the data sample of unbiased triggers.

The BESS spectrometer was flown 1998 July 29-30 from Lynn Lake, Manitoba, Canada. It floated at an altitude of 37 km (residual atmosphere of 5 g/cm^2) with a cutoff rigidity of 0.5 GV or smaller. The solar activity was close to the minimum.

3. DATA ANALYSIS

In the first stage of data reduction, we selected events with a single track fully contained inside a fiducial volume defined by the central four columns out of eight columns in the JET chamber. This definition of the fiducial volume reduced the effective geometrical acceptance down to $\sim 1/3$ of the full acceptance, but it ensured the longest track-fitting and thus the highest resolution in the rigidity measurement. The single-track selection eliminated rare interacting events. In order to verify the selection, events were scanned randomly in the unbiased trigger sample, and it was confirmed that 995 out of 1,000 visually-identified single-track events passed this selection criteria and interacting events were fully eliminated. Thus, the track reconstruction efficiency was 99.5 ± 0.2 % for a single-track event. In order to assure accuracy of the rigidity measurements, event quality such as χ^2 in the track fitting procedure was imposed on the single-track events. The efficiency of this quality-check was estimated from loose cuts of the flight data to be 93.8 ± 0.3 % and 93.0 ± 0.9 % for protons and helium nuclei, respectively. It was almost constant over the whole energy range.

In the final stage of data reduction, particle identification was performed as shown in Figure 3 by requiring proper dE/dx and $1/\beta$ as a function of rigidity. According to a study of another sample of 5×10^5 protons and 4×10^4 helium nuclei selected by using independent information of energy loss inside the JET chamber, the dE/dx selection efficiencies were 99.3 ± 0.2 % for protons and 98.2 ± 0.7 % for helium nuclei, and the contamination probabilities should be less than 3×10^{-5} for protons and 4×10^{-4} for helium nuclei. Since the $1/\beta$ distribution is well described by Gaussian and the half width of $1/\beta$ selection band was set at 3.89 σ, the efficiency is very close to unity (99.99 % for pure Gaussian).

Very clean proton samples were obtained below 3 GV. However, deuterons started to contaminate the proton band around at 3 GV, where the contamination was observed to be 2 %. No subtraction was made for this contamination, because it was as small as the statistical errors and a deuteron-to-proton ratio decreases with energy (Seo et al. 1997) following a decrease in escape path lengths of primary cosmic-ray nuclei (Engelmann et al. 1990). In conformity with previous experiments, all doubly charged particle were treated as ^{4}He. With the data reduction described above, 826,703 protons and 77,325 helium nuclei were finally identified. The combined efficiencies were 92.7 ± 1.0 % for protons and 90.8 ± 1.5 % for helium nuclei.

The geometrical acceptance defined for this analysis was calculated to be 0.0851 ± 0.0003 m^{2}sr for energetic particles by using simulation technique (Sullivan 1971). The simple cylindrical shape and the uniform magnetic field make it trivial to determine the acceptance precisely. The error arises from uncertainty of the detector alignment within 1 mm. The ratio of live data-taking-time was measured exactly to be 86.4 % by counting 1 MHz clock pulses.

The energy of each particle at the top of the atmosphere can be calculated by summing up the ionization energy losses with tracing back the event trajectory. Detection efficiencies were studied by using Monte Carlo (M.C.) simulation. The M.C. code was developed to incorporate detailed description of various interactions of helium nuclei into GEANT (Brun et al. 1994), where the cross-sections and angular-distributions of the nuclear interactions were evaluated by fitting experimental data (Bizard et al. 1977; Abdurakhimov et al. 1981; Gasparyan et al. 1982; Ableev et al. 1985; Grebenjuk et al. 1989; Glagolev et al. 1993; Abdullin et al. 1994) to energy dependent empirical formulas (Bradt & Peters 1950). The electromagnetic processes, mainly due to δ–rays, are also treated properly. They are more significant in helium nuclei interactions, because cross-sections in electromagnetic processes (σ_{em}) behaves as $\sim Z^2$ whereas those in hadronic processes (σ_{had}) is approximately proportional to $(2Z)^{2/3}$. The M.C. well reproduced the observed event shape. The simulated and observed number of hit-counters in the bottom TOF hodoscope, for instance, were agree within a discrepancy of 0.9 % and 1.8 % for proton and helium, respectively. The systematic errors in the M.C. originate mainly in uncertainties of σ_{had} and σ_{em}. We attributed relative errors of ± 5 % to $\sigma_{had}(\mathrm{p} + \mathrm{A})$, ± 5 % to $\sigma_{em}(\mathrm{p} + \mathrm{A})$, ± 15 % to $\sigma_{had}(\mathrm{He} + \mathrm{A})$, ± 20 % to $\sigma_{em}(\mathrm{He} + \mathrm{A})$, and ± 20 % to $\sigma_{had}(\mathrm{CNO} + \mathrm{A})$. Another source of a systematic error in the M.C. was the uncertainty of the material distribution inside the BESS spectrometer, which was estimated to be ± 10 %. The probability that cosmic-ray protons and helium nuclei, respectively, can pass through the whole detector without interaction was 87.6 ± 2.3 % and 74.5 ± 6.8 % at 1 GeV, and 79.7 ± 2.9 % and 64.6 ± 7.5 % at 100 GeV.

According to similar M.C. studies, the probabilities that primary cosmic-rays can penetrate the residual atmosphere of 5 g/cm^2 is about 94 % and 90 % for the proton and helium, respectively, over the entire energy range discussed here. Atmospheric secondary protons, which account for about 3.5 % at 1 GeV and less than 1.5 % above 10 GeV of observed protons, were subtracted based on the calculation by Papini et al. (1996). Atmospheric secondary helium above 1 GeV/nucleon is dominated by fragments of heavier cosmic-ray nuclei (mainly Carbon and Oxygen). The flux ratio of atmospheric secondary helium to primary C+O was calculated to be 0.14 at a depth of 5 g/cm^2, based on the total inelastic cross-sections of CNO + Air interactions and the helium multiplicity in $^{12}\mathrm{C} + \mathrm{CNO}$ interactions (Ahmad et al. 1989). The total correction of atmospheric secondary helium due to all nuclei with $Z > 2$ was estimated to be about 2 % over the entire energy range. The ambiguity in this estimation arises from the uncertainties in $\sigma_{had}(\mathrm{CNO} + \mathrm{A})$ and in absolute fluxes of heavier cosmic-ray nuclei, to which we attributed relative error of ± 20 %. The systematic errors originating in the correction of the residual air effect were estimated to be ± 0.3 % for protons and ± 2.0 % helium nuclei.

Because of the finite resolution in rigidity measurement, and the very steep spectral shape, the observed spectrum shape may suffer deformation. The effect of finite resolution was estimated by simulation, where the error in rigidity measurement was tuned to reproduce the distribution shown in Figure 2. The effect was found to be smaller than 1 % below 25 GV, but it became visible with increasing rigidity. The observed spectrum gradually gets lower than original spectrum, with a ratio of -2.5 % at 70 GV and then rapidly rises to ± 0 % around 120 GV. No correction was made for this deformation, because the effect is as small as the statistical errors over the energy range discussed here.

4. EXPERIMENTAL RESULTS AND CONCLUSION

The proton and helium fluxes at the top of the atmosphere have been obtained from the BESS–98 flight data as summarized in Table 1 and as shown in Figure 4 in comparison with the previous experiments. The first and second errors in Table 1 represent statistical and systematic errors, respectively. The overall errors including both errors are less than ± 5 % for protons and ± 10 % for helium nuclei. The dotted lines in Figure 4 indicate the spectra assumed in the calculation of atmospheric neutrinos (Honda et al. 1995). Our results, as well as other recent measurements, are favorable to lower fluxes than the ones assumed in the atmospheric neutrino calculation especially above a few tens of GeV. It may suggest an importance of the reconsideration for the atmospheric neutrino flux predictions. Precise measurements of primary cosmic-rays will help to improve the accuracy in the atmospheric neutrino calculations.

The authors would thank NASA and NSBF for the balloon flight operation. This experiment was supported by Grants-in-Aid from Monbusho and Heiwa Nakajima Foundation in Japan and by NASA in the U.S.A. The analysis was performed with the computing facilities at ICEPP, University of Tokyo.

REFERENCES

Abdullin, S. K. et al. 1994, Nucl. Phys. A, 569, 753, and references therein

Abdurakhimov, A. K. et al. 1981, Nucl. Phys. A, 362, 376, and references therein

Ableev, V. G. et al. 1985, Acta Phys. Pol. B, 16, 913, and references therein

Ahmad, M. S. et al. 1989, Nucl. Phys. A, 499, 821

Ajima, Y. et al. 2000, Nucl. Instr. and Meth. A, 443, 71

Alcaraz, J. et al. 2000, Phys. Lett. B, 472, 215

Asaoka, Y. et al. 1998, Nucl. Instr. and Meth. A, 416, 236

Bellotti, R. et al. 1999, Phys. Rev. D, 60, 052002

Bizard, G. et al. 1977, Nucl. Phys. A, 285, 461, and references therein

Boezio, M. et al. 1999, ApJ, 518, 457

Bradt, H. L., & Peters, B. 1950, Phys. Rev., 77, 54

Brun, R. et al. 1994, GEANT – Detector Description and Simulation Tool, CERN program library, CERN

Buckley, J. et al. 1994, ApJ, 429, 736

Engelmann, J. J. et al. 1990, A&A, 233, 96

Gasparyan, A. P. et al. 1982, Yad. Fiz., 36, 690

Grebenyuk, O. G. et al. 1989, Nucl. Phys. A, 500, 637, and references therein

Glagolev, V. V. et al. 1993, Z. Phys. C, 60, 421, and references therein

Golden, R. L. et al. 1991, Nucl. Instr. and Meth. A, 306, 366

Hof, M. et al. 1994, Nucl. Instr. and Meth. A, 345, 561

Honda, M. et al. 1995, Phys. Rev. D, 52, 4985

Menn, W. et al. 1997, Proc. 25th ICRC(Durban), 3, 409

Orito, S. 1987, Proc. ASTROMAG Workshop, KEK Rep., 87-19, 111

Papini, P. et al. 1993, Proc. 23rd ICRC(Calgary), 1, 579

Papini, P. et al. 1996, IL Nuovo Cimento, 19C, 367

Ryan, M. J. et al. 1972, Phys. Rev. Lett., 28, 985

Seo, E. S. et al. 1991, ApJ, 378, 763

Seo, E. S. et al. 1997, Proc. 25th ICRC(Durban), 3, 373

Smith, L. H. et al. 1973, ApJ, 180, 987

Sullivan, J. D. 1971, Nucl. Instr. and Meth., 95, 5

Webber, W. R. et al. 1987, Proc. 20th ICRC(Moscow), 1, 325

Yamamoto, A. et al. 1994, Adv. Space Res., 14, 75

This preprint was prepared with the AAS LaTeX macros v5.0.

Table 1. Proton and helium fluxes at the top of the atmosphere.

Energy Range [GeV/n]		Proton			Helium		
		$\overline{E_k}$ [GeV/n]	Flux $\pm$ ΔFlux$_{sta}$ $\pm$ ΔFlux$_{sys}$ [m^{-2}sr^{-1}sec^{-1}(GeV/n)$^{-1}$]		$\overline{E_k}$ [GeV/n]	Flux $\pm$ ΔFlux$_{sta}$ $\pm$ ΔFlux$_{sys}$ [m^{-2}sr^{-1}sec^{-1}(GeV/n)$^{-1}$]	
1.00	1.17	1.08	$8.92 \pm 0.12 \pm 0.22$	$\times 10^{2}$	1.08	$8.21 \pm 0.26 \pm 0.62$	$\times 10$
1.17	1.36	1.26	$7.72 \pm 0.11 \pm 0.19$	$\times 10^{2}$	1.26	$6.57 \pm 0.22 \pm 0.50$	$\times 10$
1.36	1.58	1.47	$6.74 \pm 0.09 \pm 0.17$	$\times 10^{2}$	1.47	$5.46 \pm 0.19 \pm 0.41$	$\times 10$
1.58	1.85	1.71	$5.46 \pm 0.08 \pm 0.14$	$\times 10^{2}$	1.71	$4.38 \pm 0.15 \pm 0.33$	$\times 10$
1.85	2.15	2.00	$4.52 \pm 0.07 \pm 0.11$	$\times 10^{2}$	2.00	$3.29 \pm 0.12 \pm 0.25$	$\times 10$
2.15	2.51	2.33	$3.63 \pm 0.05 \pm 0.09$	$\times 10^{2}$	2.33	$2.69 \pm 0.10 \pm 0.21$	$\times 10$
2.51	2.93	2.71	$2.83 \pm 0.04 \pm 0.07$	$\times 10^{2}$	2.71	$1.90 \pm 0.08 \pm 0.15$	$\times 10$
2.93	3.41	3.16	$2.22 \pm 0.04 \pm 0.06$	$\times 10^{2}$	3.15	$1.38 \pm 0.07 \pm 0.11$	$\times 10$
3.41	3.98	3.68	$1.71 \pm 0.03 \pm 0.05$	$\times 10^{2}$	3.68	$1.12 \pm 0.05 \pm 0.09$	$\times 10$
3.98	4.64	4.30	$1.27 \pm 0.02 \pm 0.03$	$\times 10^{2}$	4.30	$8.65 \pm 0.44 \pm 0.66$	
4.64	5.41	5.01	$9.65 \pm 0.19 \pm 0.26$	$\times 10$	5.01	$5.80 \pm 0.34 \pm 0.44$	
5.41	6.31	5.84	$6.89 \pm 0.15 \pm 0.19$	$\times 10$	5.84	$4.27 \pm 0.27 \pm 0.33$	
6.31	7.36	6.81	$4.91 \pm 0.02 \pm 0.20$	$\times 10$	6.80	$2.96 \pm 0.04 \pm 0.24$	
7.36	8.58	7.94	$3.43 \pm 0.01 \pm 0.14$	$\times 10$	7.92	$1.99 \pm 0.03 \pm 0.16$	
8.58	10.0	9.25	$2.42 \pm 0.01 \pm 0.10$	$\times 10$	9.24	$1.44 \pm 0.03 \pm 0.12$	
10.0	11.7	10.8	$1.70 \pm 0.01 \pm 0.07$	$\times 10$	10.8	$9.98 \pm 0.20 \pm 0.81$	$\times 10^{-1}$
11.7	13.6	12.6	$1.18 \pm 0.01 \pm 0.05$	$\times 10$	12.6	$6.82 \pm 0.15 \pm 0.55$	$\times 10^{-1}$
13.6	15.8	14.6	$8.05 \pm 0.04 \pm 0.33$		14.6	$4.50 \pm 0.12 \pm 0.36$	$\times 10^{-1}$
15.8	18.5	17.1	$5.57 \pm 0.03 \pm 0.23$		17.1	$3.16 \pm 0.09 \pm 0.26$	$\times 10^{-1}$
18.5	21.5	19.9	$3.78 \pm 0.03 \pm 0.16$		19.9	$1.99 \pm 0.07 \pm 0.16$	$\times 10^{-1}$
21.5	25.1	23.2	$2.51 \pm 0.02 \pm 0.10$		23.2	$1.51 \pm 0.05 \pm 0.12$	$\times 10^{-1}$
25.1	29.3	27.1	$1.67 \pm 0.01 \pm 0.07$		27.0	$9.15 \pm 0.39 \pm 0.74$	$\times 10^{-2}$
29.3	34.1	31.5	$1.10 \pm 0.01 \pm 0.05$		31.5	$5.98 \pm 0.29 \pm 0.49$	$\times 10^{-2}$
34.1	39.8	36.8	$7.35 \pm 0.08 \pm 0.31$	$\times 10^{-1}$	36.9	$4.30 \pm 0.23 \pm 0.35$	$\times 10^{-2}$
39.8	46.4	42.9	$4.87 \pm 0.06 \pm 0.20$	$\times 10^{-1}$	42.9	$2.65 \pm 0.17 \pm 0.22$	$\times 10^{-2}$
46.4	54.1	50.0	$3.22 \pm 0.05 \pm 0.14$	$\times 10^{-1}$	49.8	$1.88 \pm 0.13 \pm 0.16$	$\times 10^{-2}$
54.1	63.1	58.3	$2.10 \pm 0.04 \pm 0.09$	$\times 10^{-1}$	...	...	
63.1	73.6	67.9	$1.36 \pm 0.03 \pm 0.06$	$\times 10^{-1}$	...	...	
73.6	85.8	79.3	$9.17 \pm 0.20 \pm 0.39$	$\times 10^{-2}$	...	...	
85.8	100.	92.6	$6.08 \pm 0.15 \pm 0.26$	$\times 10^{-2}$	...	...	
100.	117.	108.	$4.00 \pm 0.12 \pm 0.17$	$\times 10^{-2}$	...	...	

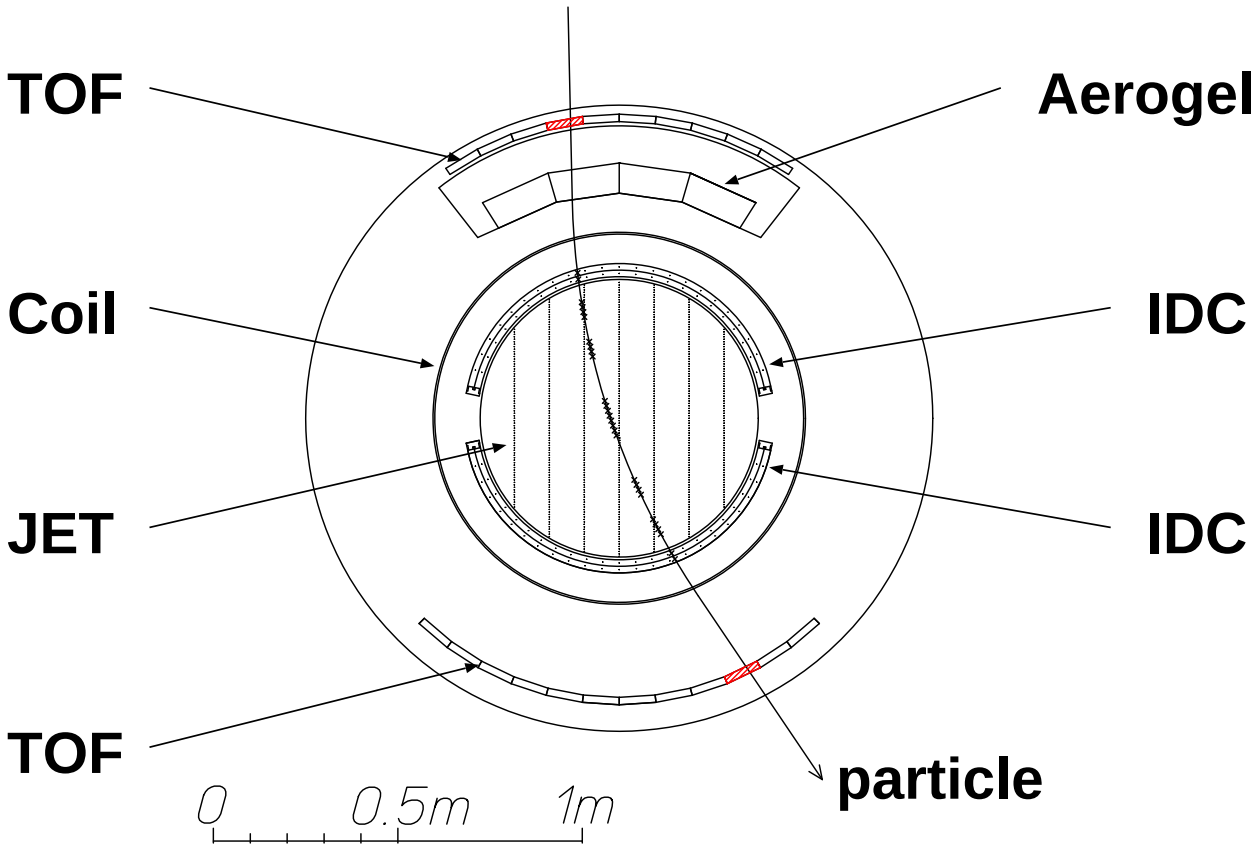

Fig. 1.— Cross-sectional view of the BESS instrument.

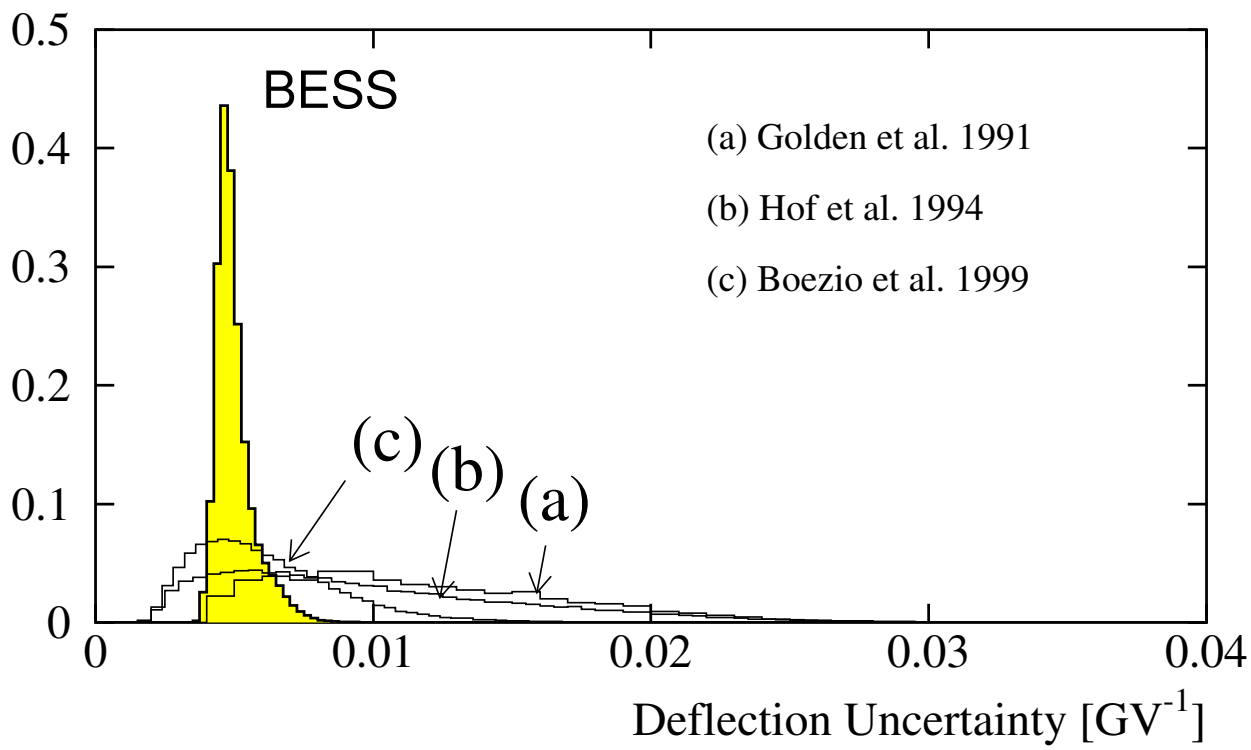

Fig. 2.— Deflection uncertainty for protons. Each area of the histogram is normalized to unity.

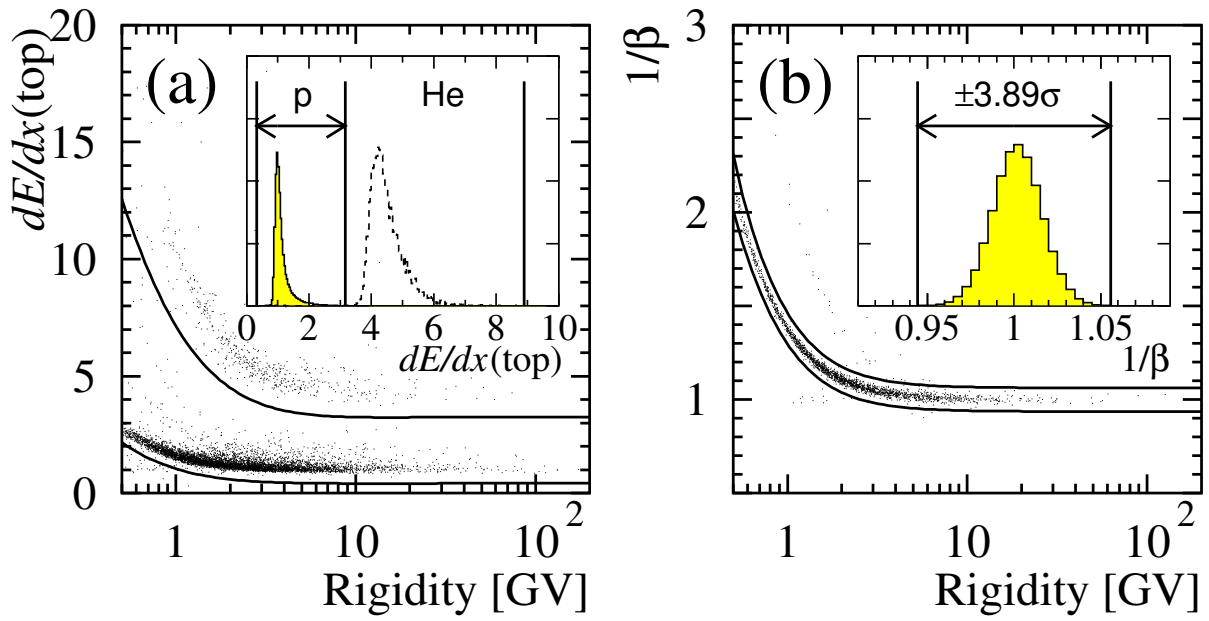

Fig. 3.— Proton bands in (a) dE/dx (top-TOF) vs rigidity plane; and (b) $1/\beta$ vs rigidity plane after proton dE/dx selection. dE/dx in the bottom-TOF is also checked. The superimposed graphs show the proton selection criteria above 10 GV. Helium nuclei were selected in the same manner.

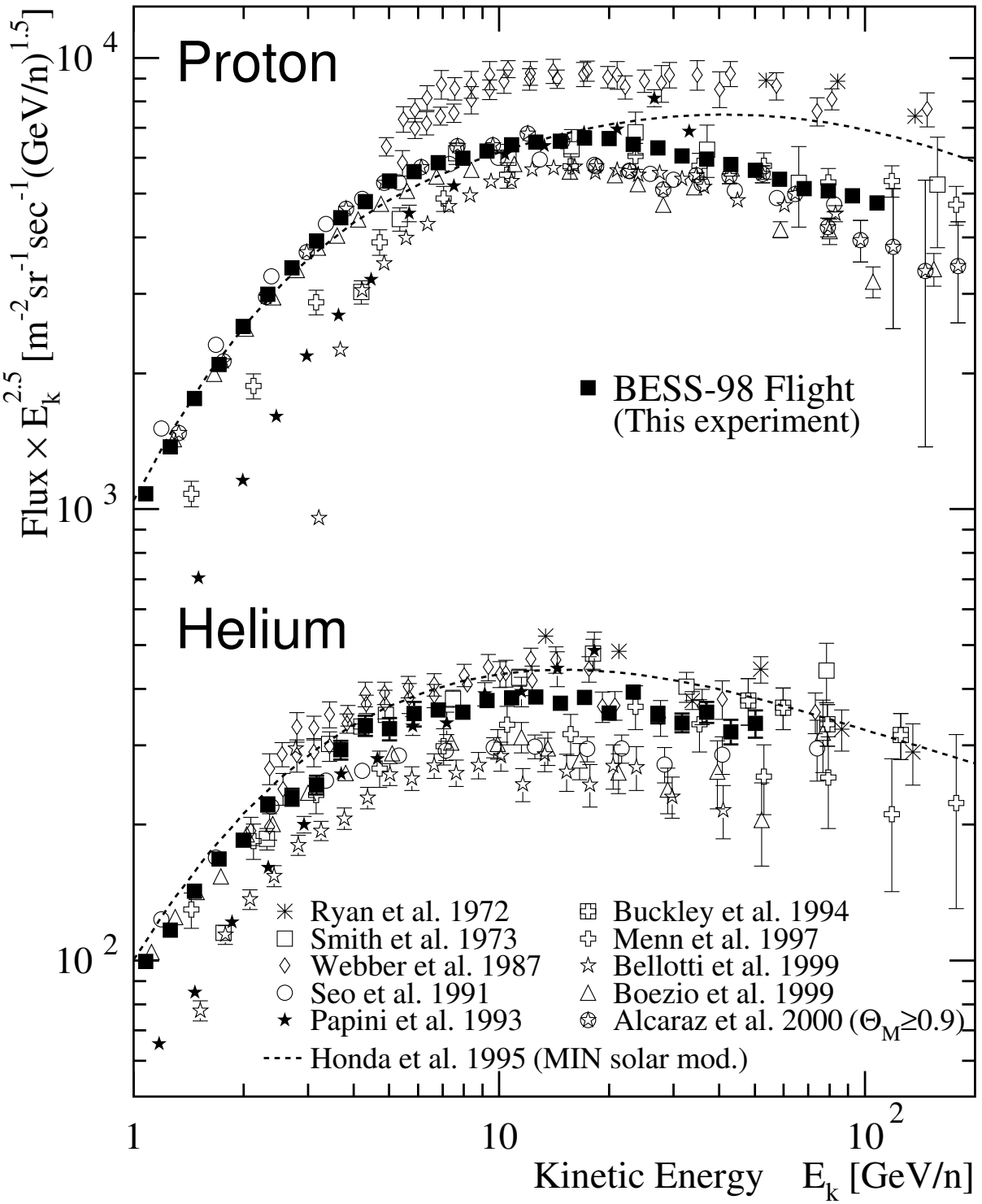

Fig. 4.— Absolute differential proton and helium spectra. Filled squares show results of the BESS–98 experiment. The spectra obtained by other experiments are also shown by different symbols indicated in the figure. Dashed lines show assumed spectra in the atmospheric neutrino flux calculation.